Hindawi Publishing Corporation

International Journal of Navigation and Observation

International Journal of Navigation and Observation
Volume 2008 (2008), Article ID 246703, 14 pages
doi:10.1155/2008/246703

Research Article

Design of Short Synchronization Codes f Future GNSS System

Surendran K. Shanmugam,[1] Cécile Mongrédien,[1] John Nielsen,[2] an

[1]Department of Geomatics Engineering, University of Calgary, AB,
[2]Department of Electrical and Computer Engineering, University of
1N4, Canada

Received 4 August 2007; Accepted 7 February 2008

Academic Editor: Olivier Julien

Abstract

The prolific growth in civilian GNSS market initiated the moderniz
to the potential deployment of Galileo and Compass GNSS system.
structure innovations to ensure better performances over legacy
synchronization codes is one among these innovations that pl
synchronization, and narrowband interference protection. In this
design based on the optimization of judiciously selected performa
obtained for lengths up to 30 bits through exhaustive search an
More importantly, the presence of better synchronization codes ov
the benefits and the need for short synchronization code design.

1. Introduction

The legacy global positioning system (GPS) has performed well be
impediments in the view point of new civilian GPS applications.
decade to satisfy the demands of these new civilian application
second-generation global navigation satellite systems (GNSSs). Th

and the restoration of Russian global navigation satellite system (
initiative, is well positioned to benefit from the three decades of GI
GNSS community has witnessed yet another highpoint with the la
Chinese Compass GNSS system [2].

A major milestone in the modernization initiative is the inclusion (
of frequency diversity besides accuracy and availability improve
numerous structural innovations that will provide the foremos
modernized signals encompass key innovations such as data-less (
secondary spreading code structure, and new modulations sche
systems utilize secondary short synchronization codes to accomplis

(i) data symbol synchronization,
(ii) spectral separation,
(iii) narrowband interference protection.

For instance, the use of short 10-bit and 20-bit Neuman-Hofman (
issue of data symbol synchronization. Besides, the different code p
channels readily provides the necessary spectral separation. The
the correlation suppression performance of the primary pseudo
spectral lines of primary PRN I5/Q5 codes thereby reducing the ef
[4]. The Galileo system also utilizes short secondary synchron
aforementioned tasks [7]. Table 1 lists the secondary code assignn

Table 1: Secondary code assignment in GPS a

The secondary synchronization codes are predominantly memory c
were obtained through truncated m-sequences (1 – 63) and gold
between memory codes and codes that are obtained from linear fe
the LFSR-based codes are appealing in the view point of hardw
lengths. The use of truncation technique can alleviate this issue a
the other hand, memory codes can be obtained for any specifi
However, exhaustive search of optimal synchronization code becon

A limitation arising due to the usage of short synchronization co
especially in the presence of frequency errors. For instance, the vu
of Doppler uncertainties is discussed in [9]. The isolation of the m
degrade from the nominal 14 dB to 4.8 dB level under worst ca
the NH code acquisition of weak GPS L5 signals becomes more diff
The existence of better synchronization codes over standardized N
on the 20-bit synchronization code originally proposed in [11]. Und
(known as the Merten's code) showed an improvement of aroun
of correlation suppression [10]. However, the performance improv
to a specific Doppler scenario and thus does not reflect the
uncertainty. Interestingly, the importance of spreading code s
corresponding measures was identified in [12]. Besides, it is also
that offer better resistance to residual Doppler errors. In this pa
such as peak-to-side lobe ratio (PSLR) and integrated side lobe r
codes that are utilized in GNSS system. More importantly, new
obtained using these performance measures through exhaustive s
proposed synchronization codes are also compared with standard
Besides, the association of the optimal synchronization codes with
codes is also established. Numerical simulations were used to de

the proposed short synchronization codes over standardized coc
measure.

The remainder of this paper is organized as follows. In Section 2,
further established in the view point of GPS L5 NH code acquisit
NH20 code in comparison to Merten’s 20-bit code under differ
measures pertaining to optimal binary periodic synchronization c
search strategy and the various code construction methods are
synchronization codes are compared with the standardized codes.
in Section 5. The final concluding remarks are made in Section 6.

2. Need for Improved Synchronization Codes

An issue with short synchronization codes is limited correlation
length. For instance, the correlation suppression performance of
from the nominal 14 dB in the presence of Doppler uncertainty |
9.2 dB for NH20 code under specific Doppler scenarios. To furthe
E1c CS25 code correlation outputs for different Doppler bins are pl
1 was obtained following the analysis reported in [10]. For insta
NH20 and CS25 code was set to 12 Hz; and this residual Dopple
25 Hz.

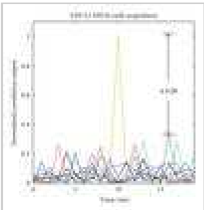

Figure 1: Superposition of secondary code cor
GPS L5 NH20 code (RHS) Galileo E1c CS25 coc

In Figure 1, we can readily observe the degradation in correlation
dB to 4.8 dB as reported earlier in [10]. On the other hand, the
18.4 dB down to 5.5 dB. The additional 3 dB degradation in CS
coherent integration time (i.e., 25 millie seconds rather than 20 m
in the original CS25 code. Accordingly, the acquisition of weak GP
in the presence of strong GPS L5 and Galileo E1c signals from
performance can be improved with longer length codes, judicial s
correlation suppression for the same code length. For examp
suppression gain of around 2 dB for Merten’s code over standa
LHS plot in Figure 2 shows the superposition of the Merten’s 20-
for the same Doppler setting as in Figure 1. The RHS plot show
standardized NH20 and the M20 code for various residual Doppler
Hz in steps of 25 Hz.

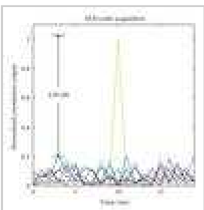

Figure 2: (LHS) Superposition of secondary co
for M20 code (RHS) PSLR performance as a fur

The RHS plot in Figure 2 readily shows the 2 dB improvement ac

NH20 code for the residual Doppler of 12 Hz. In other words, the Doppler for the same PSLR of 4.8 dB achieved by the NH20 code. improvement of around 1.7 dB over the NH20 code for the improvement in M20 code can readily be accredited to its better correlation of the different synchronization codes of length 20 (see

$$R_{\mathrm{NH10}} = \{10,-2,2,-2,-2,2,-2,-2,2,\cdot$$
$$R_{\mathrm{NH20}} = \{20,0,0,0,0,0,-4,0,4,0,-4$$
$$R_{\mathrm{CS20}} = \{20,0,0,0,0,0,4,0,-4,0,-4$$
$$R_{\mathrm{M20}} = \{20,0,0,0,0,-4,0,-4,0,0,0$$

The periodic correlation output of the M20 code, R_{M20}, has lesser to both NH20 and CS20 codes. Accordingly, one can expect its co the presence of residual Doppler. It is worth emphasizing here that exhaustive search, whereas the M20 code was obtained through NH20, M20, and CS20 corroborates the presence of multiple so search for periodic code is expected to yield multiple solutions Hence, it is necessary to obtain the binary codes that satisfy the op possible code judiciously using relevant performance measures.

Table 2: Optimal binary synchronization code

3. Optimal Synchronization Code—Figure of Merits

Better synchronization code can be obtained by optimizing the individual codes. As we are dealing with binary codes of short pe can be achieved in an exhaustive fashion. It is however, necessar readily embody the correlation characteristics of a binary code pertaining to optimal synchronization codes are the peak-to-side l ratio (ISLR) [15]. Besides, the synchronization codes are also characteristics. To define PSLR and ISLR, we first express the peri (i.e., $\mathbf{x} = [x_0, x_1, \ldots, x_{N-1}]$), at shift i, as

$$R(i) = \sum_{k=0}^{N-1} x(k)x(k-i \bmod N), \quad i =$$

where $x(k) \in \{+1, -1\}$ and $\mathbf{mod}$ is the modulo operation. The PSl correlation, $R(i)$, is given by

$$\mathrm{PSLR}(\mathbf{x}) = \frac{R(i=0)^2}{\max |R(i \neq 0)|^2}, \quad i =$$

Maximizing the PSLR measure minimizes the out-of-phase co acquisition. On the other side, ISLR measures the ratio of auto-cor energy [15]. The ISLR of a binary code is defined as

$$\mathrm{ISLR}(\mathbf{x}) = \frac{N^2}{2\sum_{i=1}^{N-1} |R(i)|^2}, \quad i = ($$

Maximizing the ISLR measure readily limits the effect of out-of-pha here that the maximization of ISLR often maximizes the PSLR m code is related to the mean value of the code and is given by

$$\mu(\mathbf{x}) = \frac{1}{N}\sum_{k=0}^{N-1} x(k$$

For binary code sets design, as in the case of OC1800 in GPS and (
mutual interference experienced by the individual codes from
correlation readily limits the effect of mutual interference between
measure embodies this mutual correlation and can be utili
optimization. For any two codes $x_p(k)$ and $x_q(k)$ of length N pertai
the mutual correlation or the MSC is given by

$$\mathrm{MSC}(p,q) = 2\sum_{i=0}^{N-1} |R_{p,q}(i)$$

where $R_{p,q}(i)$ is the periodic cross-correlation between the codes x

$$R_{p,q}(i) = \sum_{k=0}^{N-1} x_p(k)x_q(k - i \bmod N),$$

The aforementioned mean square correlation is closely related to
utilized in CDMA spread code optimization [16].

4. Optimum Code Search Results

For short code length, the synchronization code optimization ca
binary codes with optimal correlation characteristics. The develope
transform (FFT)-based block processing and matrix manipulation
ISLR were utilized for the objective maximization. Optimal synchr
through exhaustive search. Interestingly, the search process yield
on the aforementioned performance measures. Table 2 lists the
within braces, the PSLR and ISLR values, respectively.

The large number of codes arise from existence of the equivalence
periodic codes [13]. For example, the code $x(k)$, its negated vers
characterized by similar PSLR and ISLR measures. To obtain uniqu
their maximum cross-correlation is equal to the code length. Acc
following cross-correlation constraint are considered unique:

$$\max |R_{p,q}(i)| < N, \quad i = 0, 1,$$

Besides, the codes are time-reversed and hence were tested for (
included during the code selection, its significance will be emphasi
Table 2, the binary codes whose lengths are similar to the stanc
authors theoretically established the optimal periodic correlation of

$$R(i) = \begin{cases} 0 \text{ or } -4 & N \bmod 4 \\ 2 \text{ or } -2 & N \bmod 4 \end{cases}$$

The periodic correlation of optimal binary code for both odd and e
expressed below

$$R(i) = \begin{cases} 0 \text{ or } 4 \text{ or } -4 & N \bmod \\ 1 \text{ or } -3 & N \bmod \\ 2 \text{ or } -2 & N \bmod \\ -1 \text{ or } 3 & N \bmod \end{cases}$$

From (1) and (9), we see that both NH10 and M20 possess opti
code was also optimal as it satisfied the periodic correlation expr
CS20 are not optimal in the view point of (9), but can be conside
periodic correlation of NH20 does not come as a surprise as the
search [19]. It should be noted here that all the secondary codes
(i.e., sum of individual code phases is not equal to zero) and thus
the conditions for optimality. Numerical analysis later confirme
characterized by periodic correlation as predicted in (9).

All the binary codes obtained through exhaustive search indeed sa
and thereby asserting the optimality of the developed binary co
through exhaustive search resulted in similar PSLR and ISLR perfo
in accordance to (10). On the other hand, the 20-bit code obtai
performance even as the PSLR performance was the same. More
characteristics as that of M20 code introduced earlier. In Table
generally yielded better PSLR and ISLR performance. More specific
showed similar PSLR and better ISLR, even when compared to tw
The high PSLR and ISLR values observed for code lengths $N = 5,$
ideal correlation characteristics as expressed in (10). However, i
length in GNSS system can be influenced by other parameters besi

Further analysis of the optimal binary code of length 20 revealed
codes to that of the well-known Golay complementary pairs [
extensively utilized in a number of applications ranging from radar
multislit spectrometry [20]. Two binary codes $x_a(k)$ and $x_b(k)$ are
the following constraint:

$$R_G(i) = R_a(i) + R_b(i) = \left\{ \begin{array}{l} 2 \\ 0 \end{array} \right.$$

where $R_a(i)$ and $R_b(i)$ are the periodic correlation of $x_a(k)$ and x
function of the Golay complementary pair. Besides, the individual
as Golay codes. The periodic correlation in (11) immediately asser
the view point of code design. For example, the NH10 code
complementary pair as shown in Figure 3. Hence, there exists a
accomplish better acquisition abilities. Unfortunately, the NH10 c
complementary pairs.

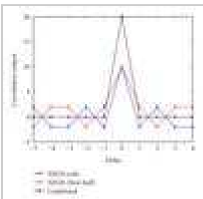

Figure 3: Correlation output of Golay complem

Motivated by this observation, the optimal binary codes of length
Golay complementary pair. Interestingly, many binary codes of le
$S20_2$ in Table 3) satisfied the Golay complementary condition. Fo
and $G10_b$ can be constructed from the even and odd samples c
give rise to Golay pairs) listed in Table 3, and the corresponding G

$$G10_a = [-1, 1, -1, 1, -1, -1$$
$$G10_b = [1, -1, -1, 1, 1, -1,$$

More importantly, the individual Golay codes $G10_a$ and $G10_b$

accordance to (9). Moreover, the Golay codes of length $N/2$ obt
optimal. Consequently, the 45 optimal binary codes of length 20 (
condition. Surprisingly, 75% (32 out of 45 codes) of the 2
complementary condition. A corollary of this conjecture indicate
length N from Golay complementary pairs of length $N/2$. The c
complementary pairs readily guarantees that every alternate
complementary correlation output of individual Golay codes. Inter
codes was utilized for signal acquisition in ultrasonic operations [2
binary code from Golay complementary pairs of length 20 (hex
binary code of length 40 (hex value "F0F6916EEE") demonstrat
Thus, it is possible to construct optimal binary codes of larger l
between optimal codes and the Golay complementary codes. Be
complementary codes readily allows for an efficient construction [2


Table 3: Secondary synchronization code—p
defined in (5), (3), and (4), resp.).

Motivated by the aforementioned observation, we constructed sy
codes of lengths 10, 20, and 25. The specific choice of code len
length 100 was divisible by 10, 20, and 25. The final code length
codes of length 10, 20, and 25 with the augmentation codes of len
and the augmentation code of length N_p and N_s. Thus, we ha
$N_p = \{10, 20, 25\}$ in our case. The final binary code, $x(k)$, of length

$$x(k) = \sum_{m=0}^{N_s-1} \sum_{n=0}^{N_p-1} x_s(m) x_p(n)$$

where $g(k)$ is the rectangular pulse function and is given by

$$g(k + \Delta T) = \begin{cases} 1 & 0 \le \Delta T \\ 0 & \text{elsew} \end{cases}$$

where T_b is the basic bit duration over which the x_k is constant
"C7F526E3FA9371FD49A7015B2"), was obtained from the prim
augmentation code, $x_s(k)$ (hex value "1"). In Table 2, we saw t
unique solutions but we only need 100 unique codes. Thus, we util
measures to limit the number of codes:

$$\text{PSLR} \ge 21.9\,\text{dB}$$
$$\text{ISLR} \ge 3\,\text{dB}.$$

The PSLR and ISLR thresholds in (15) were duly obtained from th
G100 code set [25]. Finally, the cross-correlation constraint ex
solutions. Consequently, a total number of 105 unique codes

aforementioned conditions. The hexadecimal representations of th noting here that not a single Galileo G100 code as well as the pr correlation based on (9). The following section establishes the synchronization codes in comparison to the standardized secondar

5. Acquisition Performance Analysis

Having obtained the optimal binary codes of various lengths, we n codes in comparison to the standardized codes utilized in GPS proposed in Tran and Hegarty [26] was adopted for the second assumed to be acquired within half chip duration alongside resi correlating the primary code correlation outputs with the locally Doppler was assumed to be within $\pm 250\,\mathrm{Hz}$. During the seconda searched within $\pm 250\,\mathrm{Hz}$ in steps of 25 Hz.

The Galileo CS4 code is already established as the optimal c performance analysis. Table 3 lists the $\mu(x)$, the PLSR, and the ISI proposed codes of various lengths. While the 20-bit synchronizati 10-bit codes, their ISLR performances were much better than tha there are 3 different sets of S20 code ($S20_1$, $S20_2$, and $S20_3$) and different codes are optimal in terms of correlation characteristi presence of the residual Doppler with some outperforming the o codes were not only optimal in terms of PSLR and ISLR measures the M20 and $S20_2$ over the NH20 and CS20 codes is readily ass other 20-bit codes $S20_1$ and $S20_3$ demonstrated better acquisition despite being inferior in ISLR measure. In the case of CS100 correlation protection were evaluated using a number of measure was same for both CS100 and S100 codes despite being subopti PSLR (CPSLR) measure was also obtained for CS100 and S100 c auto-correlation main peak of code ($R(i)$) to the maximum of the c

$$\mathrm{CPSLR} = \frac{R(i=0)}{\max |R_{p,q}(i}$$

Table 4 lists the maximum, minimum, mean, and the standard de Galileo CS100 and the proposed S100 codes. While the standardiz proposed S100 codes were appealing in the view point of ISLR. Th The distribution of the CPSLR and ISLR measures of the CS100 comparison. In Figure 4, we see that the standard CS100 codes codes for 50% of the times in terms of CPSLR. On the othe improvement over standard CS100 codes for 50% of the times in proposed S100 codes is inherent to its construction. Alternative multiple-objective code optimization encountered in CS100 code d

Table 4: Galileo CS100 and proposed S100 co

Figure 4: PSLR and ISLR performance of Galil

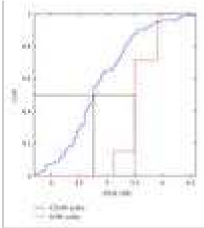

In the preceding section, we inferred the existence of multiple solu
the number of codes that accomplished the optimal correlation
arrange them, the individual codes were utilized for code acquis
obtained in the presence of residual frequency error. For example,
presence of 12 Hz residual error is plotted in Figure 5. In the cas
was relaxed to 4 dB so as to include the remaining synchroniz
performance of all the 20-bit codes (5079 codes as listed in Table
confirms the existence of optimal synchronization codes that are b
measure. However, a question may arise on the specific Doppler
performance. Further analysis did confirm this conjecture due to tl
Doppler scenarios.

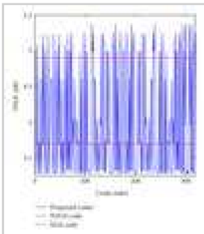

Figure 5: PSLR performance in the presence c
code.

Thus, the average of the PSLR over a range of Doppler (namely f
criterion for code selection. Under the new average PSLR measure
suppression are listed in Table 5. The S10 and $S20_1$ codes achieve
PSLR taken over a range of Doppler' s. It should be emphasized l
asserting the significance of the balanced property introduced ea
standard, Merten' s and the proposed 10-bit and 20-bit synchron
the absence of background noise. The residual Doppler was search
as reported in [10].

Table 5: Hexadecimal representation GPS/Ga
colour represents equivalence).

Table 6: Hexadecimal representation of propo

Figure 6: Effect of residual Doppler on second
bit code.

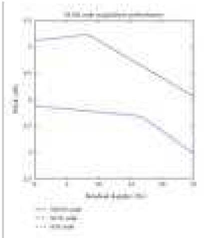

The LHS plot in Figure 6 readily affirms the limitation of standard and the proposed S10 code. Later it will be shown that the propos M10 code in the presence of frequency offset. Amongst the 20 performance in accordance to result shown in Figure 5. Both the same performance as they belong to the same equivalence class. as that of the NH20 code. Finally, the proposed $S20_1$ code show Doppler conditions. The $S20_1$ code although suboptimal in terms (property.

The correlation performance degradation in NH20 code as a func further validate this initial observation and also to compare the cc codes, numerical simulations were carried out. Figure 7 shows synchronization codes as a function of frequency offset. For the 1(the proposed S10 code over the M10 and NH10 codes. In the cas codes performed better in comparison to the M20, $S20_1$, and $S20_2$ overall best performance and readily showed a PSLR gain of arou However, the $S20_1$ is still attractive as it yielded the best PSLF aforementioned analysis for a similar setting was carried out for tl the proposed $S20_1$ and $S20_2$ codes. Note that the M25 and CS25 perform similar. Figure 8 shows the effect of residual Dopple performance as a function of frequency offset.

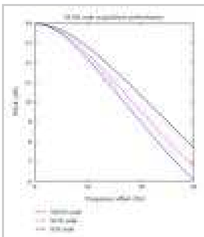

Figure 7: PSLR performance in the presence (code.

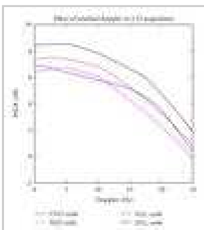

Figure 8: 25-bit code performance. (LHS) acquisition (RHS) PSLR performance as a funct

The standard CS25 code and that of M25 code were exactly same the standard CS25 resulted in better PSLR performance as shown i proposed codes demonstrated superior PSLR performance. I

complementary in their PSLR performance as shown in Figure 8. I
for not only achieving better PSLR performance (around 2 dB) ir
similar PSLR performance to that of standard CS25 code for a wide

Finally, the code acquisition performance of the standard CS100 ar
similar manner. The residual Doppler range was reduced to 7.5
utilized in acquiring these codes. Figure 9 shows the average PS
codes. The standard CS100 code demonstrated better performance
settings. The proposed code despite being characterized by better
method from code of short length. Nevertheless, it readily corr
multiple code design problem.

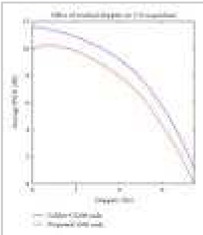

Figure 9: 100-bit code performance. (LHS) acquisition (RHS) PSLR performance as a funct

6. Conclusions

The design of secondary synchronization code for GNSS syster
tracking. A limitation arising due to the usage of short secondar
isolation especially in the presence of residual frequency errors
measures that can be utilized for secondary synchronization coc
measures were utilized to obtain optimal codes of various lengths
the association between the optimal codes and the systematic
proposed secondary synchronization codes of lengths 10, 20, anc
superior correlation isolation performance in the presence of resi
although appealing in terms of ISLR measure demonstrated inferic
codes. Truncation of LFSR codes or code design using genetic
correlation characteristics. The significance of the correlation i
synchronization codes in terms of probability of false alarm and
judicious design of short synchronization codes can offer opti
generation.

Example 1. The NH10 Code represented by the hexadecimal value

$$F \rightarrow 1\ 1\ 1\ 1,$$
$$2 \rightarrow 0\ 0\ 1\ 0,$$
$$8 \rightarrow 1\ 0\ 0\ 0.$$

Hence, "F28" $\rightarrow 1, 1, 1, 1, 0, 0, 1, 0, 1, 0, 0, 0$. The last two digits
symbols are mapped in to -1. (i.e., $0 \rightarrow -1$).

References

1. G. W. Hein, J. Godet, J. L. Issler, et al., "Status of Galileo fi *15th International Technical Meeting of the Satellite Division* 266, Portland, Ore, USA, September 2002.

2. T. Grelier, J. Dantepal, A. Delatour, A. Ghion, and L. Ries, “
satellite signals,” *Inside GNSS*, 39 pages, June 2007.

3. R. D. Fontana, W. Cheung, and T. Stansell, “The moderniz
September 2001.

4. A. J. van Dierendonck and C. Hegarty, “The new L5 civil GF
2000.

5. B. C. Barker, K. A. Rehborn, J. W. Betz, et al., “Overview o
National Technical Meeting of the Institute of Navigation (IO
2000.

6. S. Pullen and P. Enge, “A civil user perspective on near-ter
Proceedings of the GPS/GNSS Symposium, p. 11, Tokyo, Ja

7. Galileo SIS ICD, “Galileo Open Service: Signal In Space Int

8. J. J. Rushanan, “The spreading and overlay codes for the L
Technical Meeting of the Institute of Navigation (ION NTM '0

9. L. Ries, C. Macabiau, Q. Nouvel, et al., “A software receive
International Technical Meeting of the Satellite Division of th
Portland, Ore, USA, September 2002.

10. C. Macabiau, L. Ries, F. Bastide, and J.-L. Issler, “GPS L5 r
the International Technical Meeting of the Institute of Navig
September 2003.

11. S. Mertens, “Exhaustive search for low-autocorrelation bin
18, L473 pages, 1996.

12. F. Soualle, M. Soellner, S. Wallner, et al., “Spreading code
Proceedings of the European Navigation Conference (ENC G

13. C. Tellambura, M. G. Parker, Y. J. Guo, S. J. Shepherd, and
estimation using discrete Fourier transform techniques,” *IE*
230 pages, 1999.

14. D. V. Sarwate and M. B. Pursley, “Crosscorrelation properti
Proceedings of the IEEE, vol. 68, no. 5, 593 pages, 1980.

15. M. Golay, “The merit factor of long low autocorrelation bin
Information Theory, vol. 28, no. 3, 543 pages, 1982.

16. M. Rupf and J. L. Massey, “Optimum sequence multisets fo
channels,” *IEEE Transactions on Information Theory*, vol. 4

17. A. Lempel, M. Cohn, and W. L. Eastman, “A class of balanc
properties,” *IEEE Transactions on Information Theory*, vol.

18. D. Jungnickel and A. Pott, “Perfect and almost perfect sequ
1–3, 331 pages, 1999.

19. F. Neuman and L. Hofman, “New pulse sequences with des
IEEE National Telemetry Conference (NTC '71), p. 272, Was

20. M. Golay, “Complementary series,” *IEEE Transactions on I*

21. H. Urkowitz, “Complementary-sequence pulse radar with m

September 1992, US patent 5151702.

22. H. Minn, V. K. Bhargava, and K. B. Letaief, "A robust timing systems," *IEEE Transactions on Wireless Communications*,

23. V. Diaz, J. Urena, M. Mazo, J. J. Garcia, E. Bueno, and A. He for multi-mode ultrasonicoperation," in *Proceedings of the Technologies and Factory Automation (ETFA '99)*, vol. 1, p.

24. S. Z. Budisin, "Efficient pulse compressor for Golay comple no. 3, 219 pages, 1991.

25. European Space Agency, "Galileo Open Service: Signal In S control document, European Union, May 2006, http://www.g 20ICD%20230506.pdf.

26. M. Tran and C. Hegarty, "Receiver algorithms for the new c *Technical Meeting of the Institute of Navigation (ION NTM '0*

27. S. K. Shanmugam and H. Leung, "Chaotic binary sequence estimation," in *Proceedings of the 60th IEEE Vehicular Tech* Angeles, Calif, USA, September 2004.